

## Structural studies on gels from isotactic polystyrene

E. D. T. Atkins, M. J. Hill, D. A. Jarvis, A. Keller, E. Sarhene, and J. S. Shapiro<sup>\*)</sup>

H. H. Wills Physics Laboratory, University of Bristol, Bristol U.K.

**Abstract:** The thermoreversible gelation phenomena exhibited by isotactic polystyrene (*i*-PS) was examined in depth, utilising a variety of experimental techniques. The primary aims were identification, relationship, description and visualisation of the morphologies corresponding to the two types of crystallization as diagnosed by the different crystal structures revealed by X-ray diffraction. While centred on electron microscopy the investigation used X-ray and electron diffraction, differential scanning calorimetry and Fourier transform infra-red spectroscopy in combination. A satisfactory correlation between all these techniques was established, including the important reassurance that the characteristics of the gel state are preserved on drying, a feature necessitated by most structure methods. The *i*-PS gel system as a whole displays particularly clearly the distinction between gel forming and chain folded lamellar crystallization and the coexistence, morphological relationship and competition between the two crystallizable species. In addition, and most significantly, the gel crystals possess a crystal structure involving extended chains, close to an all-trans conformation, which are quite different to those obtained from conventionally crystallized *i*-PS ( $3_1$  helix). This former extended conformation in itself has become the starting point for new geometric and stereochemical considerations and in addition offers a convenient diffraction based fingerprint to delineate between the two modes of crystallization. Thus the conversion of the gel crystal structure to the conventional  $3_1$  helix structure on heating could be monitored. Further, that in the processes of heat annealing, remnants of these gel fibres initiate the development and dictate the orientation of a shish-kebab type platelet growth with the  $3_1$  helix crystal structure. This conversion process has been followed by electron microscopy and supplemented infra-red spectroscopy, low angle X-ray diffraction and differential scanning calorimetry. The different roles of fibres and platelets on stretching have been identified. Conditions for the existence of the gel crystals in their different variants are specified with relevance to ongoing arguments and discussions in the subject. Further, it was established that passing through the gel phase significantly enhanced the crystallization in the conventional crystal form making the normally slowly crystallizing *i*-PS into a fast crystallizable polyolefin.

**Key words:** Isotactic polystyrene, gels, structure, morphology, conformation, X-ray diffraction, electron microscopy, DSC, FTIR, crystallization.

### Introduction

#### *Two forms of crystallization*

The present work forms part of a wide ranging activity, namely gel forming crystallization, being pursued within this laboratory (for review see 1). Within the broad topic of crystallization induced gelation from solution, it will be concerned with the behaviour of one specific polymer that of isotactic polystyrene (*i*-PS). *i*-PS has both a special and a central position in the field. Historically it was the material on which we ourselves recognized the

phenomenon of gel forming crystallization as distinct from other crystallization modes, and it has served as a model substance for the study of such crystallizations since. In addition, *i*-PS displays features characteristically of its own. These are of interest *per se*, yet their implications are confined not only to *i*-PS, or to gelation crystallization, but are of relevance to other wider issues such as the chain conformation of polyolefins.

First, the background will be briefly recapitulated, *i*-PS displays two modes of crystallization from solution: (1) it can crystallize in the form of platelets apparent as a turbid suspension, (2) it can crystallize by setting as a clear gel. Crystal types (1) and (2) form in different temperature ranges. Type (1) crystals form

<sup>\*)</sup> permanent address: School of Chemistry, Macquarie University, North Ryde, New South Wales 2113, Australia.

at the higher temperature from 130 °C down to ~ 25 °C, the crystallization rate passing through a maximum at around 60–70 °C. Type (2) crystals appear at lower temperatures typically starting to form at an appreciable rate at around 20 °C, the rate increasing with decreasing temperature. In a limited temperature range, around 20 °C both (1) and (2) crystal types can appear simultaneously resulting in a turbid gel. Alternately a composite turbid gel can be attained by not allowing type (1) crystallization to proceed to completion but interrupt crystallization by quenching to below 20 °C.

The crystalline nature of the products in either case was verified by X-ray diffraction. In the case of type (1) crystals this was self evident from the diffraction patterns of sedimented mats. In type (2) crystals X-ray diffraction patterns were obtained in the practically dried state of the gel, where both the special nature of the diffraction pattern (see later) and the combination of X-ray and Differential Scanning Calorimetry (DSC) (information from melting signals could be obtained from the gel in the same dilution as formed) confirmed that the setting of the gel was caused by the formation of crystals. Since the gels themselves were extensible, suitably shaped samples could be drawn and fibre X-ray diffraction patterns obtained. As the latter contained much more information than X-ray diffraction patterns from randomly oriented samples, they were used for all subsequent studies [2–5] and feature in the present work. Similarly the underlying oriented samples will be used for the new kind of exploration, involving electronmicroscopy and infrared spectroscopy. We believe that the use of the oriented gel samples has not detracted from the generality of the conclusions regarding the intrinsic nature of the gel forming crystals, on the contrary, enabled more information to be obtained, a point to which we shall repeatedly return to later.

The two crystallization modes denoted by crystal types (1) and (2) above are clearly distinct and can occur in competition as laid out previously (2). The principal distinctions merit recapitulation.

*a) Consistency:* Crystal type (1) is particulate, giving rise to suspensions while type (2) is in the form of a gel, a distinction apparent by visual inspection.

*b) Morphology:* in type (1) the particles are platelets containing the chains in the familiar folded conformation. In type (2) the crystals must be the agents which produce the junctions necessary to form the interconnected network responsible for gelation. This means that they must arise through the confluence of several

chains as opposed to the predominate folding of chains onto themselves as in the platelet type (1) crystals. Thus crystals of type (2) have a predominantly micellar character of essentially fibrous nature (for justification of fibrosity see reference [2] and also further evidence below).

*c) Crystal structure:* this is the most striking feature distinguishing *i*-PS from other polymers capable of crystallizing both as gels and platelets. Crystals of type (1) have the characteristic crystal structure determined by Natta, Corradini and Bassi [6] with the chains in the form of the well known three fold ( $3_1$ ) helix, ((*TG*)<sub>3</sub> sequences *T* ≡ trans, *G* ≡ gauche conformation). The gel forming crystals, type (2), display different X-ray diffraction patterns consistent with a nearly fully extended all-trans (*TT*) chain conformation. There is a small departure (21° and 13° for the backbone torsion angles) from the pure *TT* conformation (0°, 0°) leading to a highly extended helix with twelve monomer units, (or rather with 6 pairs of dimers, each dimer having pairs of torsion angles differing slightly in an alternate manner from the idealised 21° and 13° set) [5].

#### *The two crystal structures*

It will be apparent that highly extended (close to *TT*) structures in polyolefins with bulky side groups are contrary to traditional textbook knowledge which made the above conclusion rather surprising. The energetic feasibility of near extended *i*-PS chain has nevertheless been verified by work from this laboratory [4] and subsequently confirmed by others [7, 8]. The historical development of the latter issue is particularly instructive deserving special attention and will be covered in a separate paper shortly [9].

The emergence of two chain conformations is surprising enough, particularly when one of them (the nearly fully extended *TT*) seemed contrary to basic intuition. Even more puzzling is the fact that it is the latter which is always associated with gel formation, and vice versa. Two latest papers by Sundararajan [10, 11] make a specific proposition as regards the origin of the effect. According to Sundararajan the initial presence and retention or introduction of a certain type of solvent is a prerequisite for the extended (gel) structure, a point which will be one of the issues in our present paper.

It needs emphasizing that the 'crystal structure' corresponding to the new extended type version is far from solved. What is firm is the near extended *TT* chain nature and the overall helical characteristics as reflected by the layer line periodicity in the X-ray

diffraction pattern, and further the energetic feasibility of such a structure. The material of the present paper will rely on nothing more than these facts. Beyond these there are inconsistencies in the observed relative intensities of the layer lines which are apparently not simply remediable on the basis of the single chain Fourier transform calculations alone as applied so far. One of our initial X-ray diffraction patterns published of an *i*-PS gel in a particular solvent exhibited weak odd order layer line intensities (fig. 1). On the basis of this observation and model building calculations Sundararajan [7] proposed a double helical model for the *i*-PS gel structure. This model does not appear in subsequent papers [10, 11] by the same author and so we must assume that such a model is now withdrawn as a possible solution. A unit cell has in fact been proposed in the last paper by Sundararajan [11] however, as it will be shown in our companion paper [9], this is not tenable, not to speak of some serious question marks relating to underlying experimental diffraction results obtained in this work on dis-oriented patterns. As the detailed intensities, corresponding to the same layer line geometry are affected by the mode of gel preparation (solvent used) [5] there is clearly no single unique full crystal structure associated with the near extended *TT* conformation of the single chain. For this reason we ourselves have not pursued the solution or refinement of the structure further at this stage, neither will this feature in the present paper.

In what follows we shall adopt the following nomenclature. The extended type near *TT* structure we shall call 'gel structure' and the conventional crystal structure by Natta et al. [6] as ' $3_1$  structure'.

#### *Transformation of the gel to the $3_1$ helix structure*

It was recognized early that on heating, the gel structure gives place to the  $3_1$  structure [2]. The changes are gradual and within an appreciable temperature interval both structures can co-exist, the proportion of the gel structure diminishing with increasing temperature. Whether the gel structure actually transforms into the  $3_1$  structure, or whether the gel structure melts first and the  $3_1$  structure forms anew from the molten material remains an open question. So does the question as to whether the same or different portions of the material are involved in the two modes of crystallization in view of the fact that crystallinity in *i*-PS of any kind is always low (below 50%), hence there remains scope for either alternative. The issue of conversion of one structure into another will feature prominently in this paper where amongst

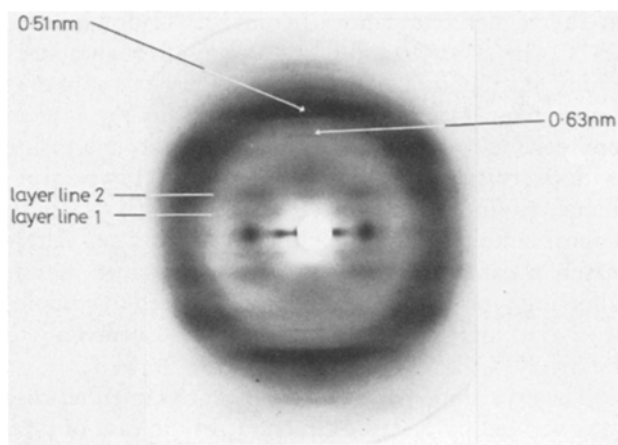


Fig. 1. X-ray fibre diffraction pattern obtained from *i*-PS trans-decalin gel. The fibre axis is vertical. The layer line spacing is 3.06 nm and note the intensity on the second layer line is greater than that on the first layer line. The strong meridional diffraction signal occurs on the sixth layer lines with spacing 0.51 nm. Note also the weaker and noticeably sharper arc at 0.63 nm which is the 300 from the  $3_1$  helix structure oriented at right angles to the fibre direction

others, rather unexpectedly, conversions between two different gel structures has also been noted.

#### *Purpose of the paper*

The principal purpose of the present work was the morphological identification of the two kinds of crystal under the electron microscope. In service of this overriding aim the condition of emergence, transformation, and/or interconversion of the two basic structures were examined in greater detail by a coordinated approach using DSC calorimetry, X-ray diffraction and infra-red spectroscopy in order to obtain full consistency between all the techniques used, at the same time utilizing the special potential of each. Further, techniques such as are applicable to bulk samples (X-rays, DSC) served as reassurance of the genuineness of our electron microscopy necessarily restricted to ultrathin specimens. Another aspect, the need or otherwise of the presence of solvents, was renewedly assessed in the light of latest papers from elsewhere [9–11] a subject which however, will not be pursued here beyond its absolute essentials. As already stated no further effort will be made in this paper to refine the structure at a molecular level.

#### **Materials**

The high molecular weight polymer (a gift from Professor Berghmanns and Dr. Lemstra) was either extracted in butanol for 24

hours or purified as follows. The polymer was dissolved in methylene chloride and after filtering under vacuum the solution was poured into excess methyl ethyl ketone and boiled for 4 hours and left to stand overnight. After evaporation of the methylene chloride the *i*-PS was precipitated from ketone leaving atactic polystyrene in solution. Thus highly stereoregular *i*-PS was obtained, characterised by  $M_n = 6.9 \times 10^4$  and  $M_w = 7.4 \times 10^5$ . The tacticity of the sample was in excess of 95% as measured by NMR.

## Methods

### Sample preparation and experimental

#### X-ray diffraction

5–10% w/w solutions of *i*-PS in the above solvents were made at dissolution temperatures in the range 150–180 °C. During the dissolution procedure dry nitrogen was flushed through the solution. The heating period was kept to a minimum by stirring the solution vigorously which removes the need for stabilizing additives which can contribute to, and hence complicate, the X-ray diffraction pattern. The *i*-PS was dissolved in a pre-heated test tube containing the solvent and after complete dissolution transferred into a preheated convoluted tube and quenched to 0 °C.

Clear gels were obtained in most of the solvents used in this study (*i*-PS in DMP yields cloudy gels). The gels were stretched at room temperature, and also in certain instances at 4 °C, by suspending a filament of the gel and hanging a load on the free end (typically in the range 5–70 g). Under these conditions the filaments reached a constant length and in a few cases were stretched further in a spring-loaded frame at room temperature. The stretch ratio of the fibres obtained varied between 1.5 to 2.7.

Gels prepared from *cis* decalin, benzyl alcohol and dimethylphthalate (DMP) solvents were found to stretch greater amounts than gels prepared from dimethylformamide (DMF) and nitrobenzene solvents. The stretched gels were used for both wide and low angle X-ray diffraction studies after extraction in solvents such as acetone, methanol and ether or by drying in a vacuum oven. The oriented *cis* decalin, *trans* decalin and benzyl alcohol prepared *i*-PS fibres were heat annealed at temperatures in the range 30–180 °C and also examined by X-ray diffraction.

Wide angle X-ray diffraction photographs were obtained using CuK $\alpha$  radiation with a nickel filter on a Phillips or Enraf sealed tube generator. Pinhole collimation was used and the X-ray cameras could be evacuated or filled with helium to reduce air scatter. Samples were dusted with calcite powder for calibration purposes. The low-angle diffraction photographs were obtained using a Rigaku-Denki point collimated camera operating on an Elliot G X 6 rotating target generator and nickel filtered CuK $\alpha$  radiation. Exposure times varied between 10 and 100 hours.

#### Electron microscopy

Four different methods of sample preparation were used and found to be essentially equivalent. Oriented annealed samples, showing the  $3_1$  helix structure, were prepared as follows:

- (1) Bulk sample (previously used for X-ray work) sectioned after annealing.
- (2) Bulk sample (X-rayed unannealed) sectioned and sections subsequently annealed in the oven.
- (3) As (2) but sections annealed in the hot stage of the electron microscope.
- (4) Thin films cast on cold decalin, subsequently stretched and annealed.

Samples prepared from *trans* decalin were viewed both with and without 'extraction' (5) for one hour with diethylether or, more usually, acetone. This extraction left the diffraction pattern unchanged but clarified the morphology, most likely by reducing occluded or bound solvent. Extraction was not carried out with samples prepared from *cis* decalin. Acetone and diethylether do change the gel material prepared from *cis* decalin, causing it to crystallize in the  $3_1$  helix form.

It proved difficult to control the thickness and degree of strain of thin films. Because of this most of the work was performed with sections which were cut to equal thickness from samples prepared under equal strains. Thin films were used as a check to identify any artefacts of sectioning. The morphologies of oriented samples reproduced in this paper are all sections. Those found in thin films were essentially the same.

Sections were cut at room temperature using a diamond knife. They were 70–90  $\mu\text{m}$  thick. Samples were cut transversely and longitudinally. Longitudinal sections were cut with the knife moving at right angles to the fibre direction. This cutting direction gave uniform, undistorted samples with a diffraction pattern similar to that obtained by X-rays at all points. Cutting sections longitudinally with the knife moving along the fibre direction gave distorted and broken sections with variable diffraction patterns.

Samples were examined in a Philips 301 transmission electron microscope. Most were mounted in a single tilt stage. Those annealed in the microscope were held in a hot stage in which the temperature could be controlled to within  $\pm 3$  °C, but the heating rate could not be adequately controlled.

#### Differential scanning calorimetry

The calorimetric measurements were performed using a Perkin Elmer DSC 2. The temperature scale was calibrated using both indium and tin. A heating rate of 20 °C/min was used. The sensitivity for the scan of oriented fibres was 1 mcJ/sec and that for the unoriented gels was 2 mcJ/sec.

#### Fourier transform infra-red

Drawn *i*-PS *cis*-decalin and *i*-PS *trans*-decalin gels were prepared in the manner described in the X-ray section above, except that the gels were in the form of thin films suitable for infra-red measurements. The two samples were annealed at successively higher temperatures, while held under constant load. After each annealing at a particular temperature the polarised infra-red spectra were recorded at room temperature.

A Nicolet model 7199 FTIR spectrometer was used to record the polarised spectra of these gels. One hundred co-added interferograms at a resolution of 2  $\text{cm}^{-1}$  were used to obtain each spectrum. The spectral subtraction capability of the FTIR spectrometer was used to remove the spectrum of any remaining solvent, in the same way as illustrated by Painter et al. [12]. This was particularly important in the case of the *i*-PS *trans*-decalin gel, since a strong solvent band at 925  $\text{cm}^{-1}$  could interfere with observation of a polymer band at 922  $\text{cm}^{-1}$  characteristic of the  $3_1$  helix structure. Also for both the *i*-PS *cis*-decalin and *i*-PS *trans*-decalin gels, solvent bands in the region of 1100 to 1050  $\text{cm}^{-1}$ , if not removed, interfere with observation of the 'gel' bands at 1061 and 1069  $\text{cm}^{-1}$ .

#### Crystal structure and orientation by X-ray diffraction

The present X-ray section falls in two categories:  
i) the existence, formation or interconversion of the

two different crystal structures ii) anomalous orientation effects.

### The two crystal structures

The effect of heating on the X-ray patterns of the gel structure has already featured in our first paper of the subject [2]. There it was stated and illustrated that heating of an oriented gel sample produces diffraction signals characteristic of the  $3_1$  helix structure, the gel and the  $3_1$  helix structure coexisting over a certain temperature interval, until at annealing at sufficiently high temperature the latter alone persisted. In the present work this aspect was examined more fully, particularly in relation to the infra-red and DSC work with which it was examined in parallel. Additional to the early work, gel samples obtained both from trans and cis decalin were investigated as a function of annealing. Diffraction patterns were taken at the elevated annealing temperature itself, in fact annealing series were carried out by raising the temperature of the sample in successive steps while mounted on the X-ray camera and the diffraction patterns recorded. It will be stated to begin with that these X-ray experiments at elevated temperature revealed the essential features in the diffraction patterns which developed on heating, and remained unaffected by subsequent cooling to room temperature. This result is important since it means that the changes occurring on heat treatments are temperature irreversible and further, that we need not distinguish between X-ray diffraction patterns taken 'hot' or 'cold', and therefore the same argument will apply to the electron microscopic observations, which is the subject to follow. In line with all the previous X-ray diffraction work the present studies were nearly all performed on oriented specimens for reasons stated in the introduction.

Figure 1 shows the diffraction patterns of pure gel structures obtained from trans decalin. As described previously the principal feature is the strong meridional diffraction signal at 0.51 nm, which is the periodicity corresponding to two monomer units in near extended conformation. It was the observation of this periodicity which was the starting point of the whole subject [2-4]. In fact the average gel preparation may not show any other prominent diffraction spacing, particularly when unoriented. The additional features in figure 1 may appear with varying distinctness dependent on preparation conditions. These features include the layer line structure as seen in figure 1, according to which the basic axial periodicity is 3.06 nm of which the 0.51 nm is the sixth order. It is on the basis of such a pattern that the near all  $TT$  helix

for the gel structure has been derived. A notable feature is the weakness in intensity of the first layer line relative to the second. This particular feature has caused problems in the interpretation of the diffraction pattern on the basis of a single, purely isotactic chain a difficulty so far unresolved.

As reported previously [4, 5] in gels prepared from cis as opposed to trans decalin the ratio of the intensity of the first two layer lines is reversed (fig. 5) that of the first being stronger than that of the second, without, however, any change in the layer line periodicity, hence in the underlying backbone geometry of the near all  $TT$  extended helical conformation. This result reinforces the inherent stability of the extended  $TT$  structure which as we expect arises from specific interactions between contiguous units, in particular the aromatic groups. As pointed out in reference [5] these differences in intensity have important potential implications, which, however, will not concern us here further beyond the fact that both of the above gel patterns feature as the starting stage of our heating series.

Figures 2, 3 and 4 illustrate stages in the heat annealing in order of ascending temperature. Figure 2 is from a sample annealed at 70 °C and still corresponds essentially to a gel structure with the first appearance of the presence of the  $3_1$  helix structure in the form of the additional sharp equatorial diffraction arcs at spacing 1.09 nm, 0.63 nm and 0.546 nm with Miller indices 110, 300 and 220 respectively. In the X-

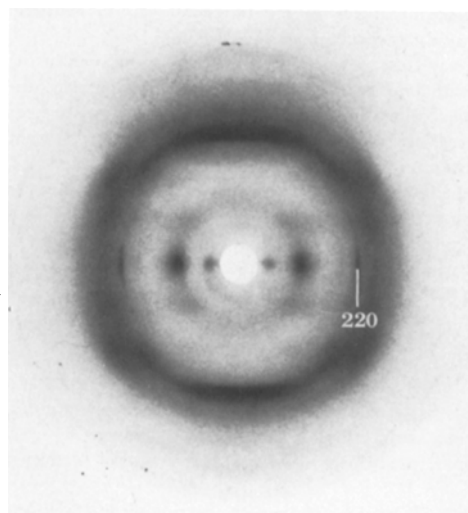


Fig. 2. X-ray fibre diffraction pattern of *i*-PS trans-decalin gel heat annealed at 70 °C. Note the additional diffraction signals appearing on the equator which represent the first appearance of the presence of the  $3_1$  helix structure (arrowed)

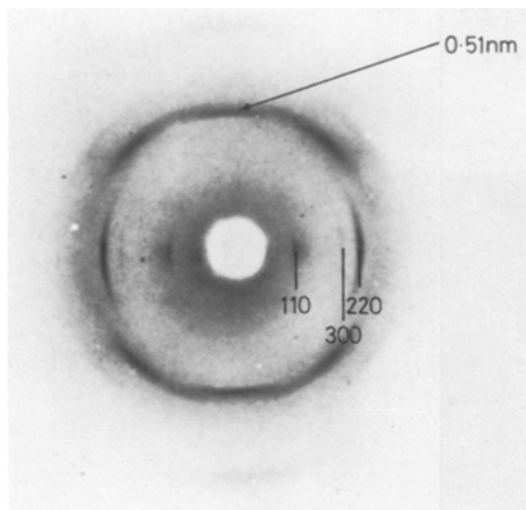


Fig. 3. X-ray fibre diffraction pattern of *i*-PS trans-decalin gel heat annealed at 100 °C and recorded at that temperature. The  $3_1$  helix structure has now become the dominant form. The 0.51 nm meridional diffraction signal (arrowed) is a horizontal streak in contrast to the arcs of the  $3_1$  helix structure.

ray diffraction pattern shown in figure 3, which is for a sample annealed at 100 °C, and taken 'hot', the  $3_1$  helix structure has become the dominant entity but with some gel structure still present (the 0.51 nm diffraction signal on the meridian, which should be noted is a streak perpendicular to the meridian in contrast to the arcs due to the  $3_1$  helix structure). Figure 4 illustrates a diffraction pattern of a sample

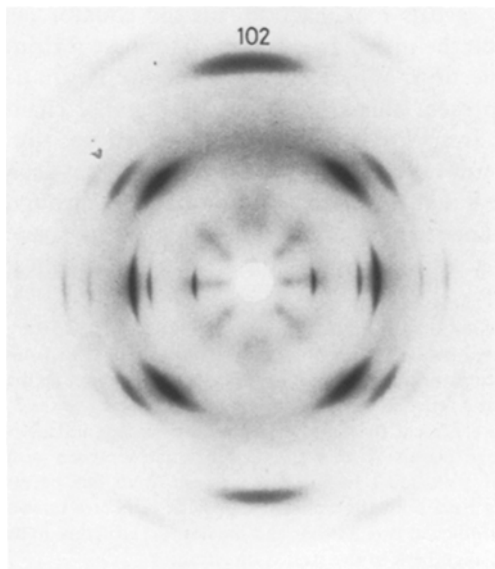


Fig. 4. X-ray fibre diffraction pattern of *i*-PS trans-decalin gel heat annealed at 150 °C. All the diffraction signals index on the  $3_1$  helix structure

annealed at 150 °C and corresponds entirely to the  $3_1$  helix structure. The temperature at which the gel structure diffraction signals disappear has not been exactly identified but it is at about 110–120 °C. It cannot be readily defined more precisely, as there is variation from one preparation to another, a variability which also extends to the relative amounts of the two structures, where both are present, at the lower annealing temperatures. Whatever the cause of this variability (possibly time of annealing, initial or residual solvent content and no doubt the differences in the intrinsic quality of the diffraction patterns) we can assert that the transformation of the diffraction pattern from that of the gel structure to the  $3_1$  helix structure closely corresponds to the region of the endo-exotherm pair in the DSC thermograms (see fig. 10 later) spanning the temperature interval of 70–140 °C, the peak values as we have seen being in the range of 90–105 °C for the endotherm and close to 120 °C for the exotherm (the endotherm peak taking on higher values as a result of annealing at temperatures below the peak value).

Using gels formed from cis-decalin a new and important observation was made. On annealing at 45 °C for 12 hours the cis decalin gel pattern (fig. 5) transformed into a pattern characteristic to the gels obtained from trans decalin (fig. 6). This observation is significant for two reasons. First, that it affects retrospectively the interpretation of the thermograms of cis decalin gel preparations [5] where the wet gel melting point was identified as 60 °C, i. e. identical to that of the gel from trans decalin. The present result

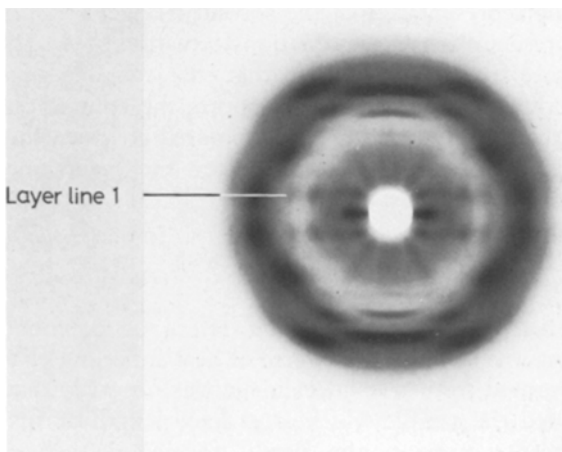


Fig. 5. X-ray fibre diffraction pattern obtained from *i*-PS cis-decalin gel. The layer line spacing is identical to the *i*-PS trans-decalin gel but note the strong intensity on the first order layer line in this case

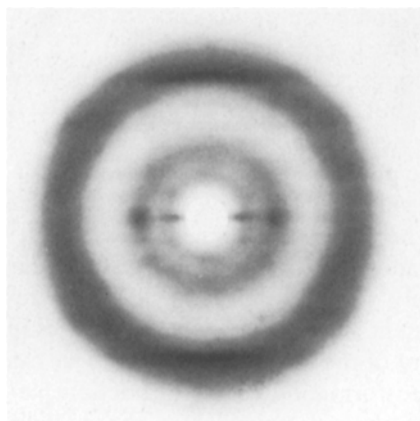


Fig. 6. X-ray fibre diffraction pattern obtained from *i*-PS cis-decalin gel heat annealed at 45 °C for 12 hours. It exhibits the characteristic features of the *i*-PS trans-decalin gel

may well imply that this 60 °C melting point would correspond to that of the wet gel from trans decalin resulting from the transformation of the cis decalin gel into the trans decalin gel structure just discovered. Indeed, current work has revealed an endotherm at about 38 °C for the gel from cis decalin which accordingly could be the true melting (or dissolution) temperature of the cis decalin gel structure. Secondly, it is to be noted that completely dry gels from cis decalin are not obtainable (they transform to the  $3_1$  helix structure) hence the melting point of the dry gel cannot be assessed *a fortiori*. The instability of the gel structure from cis decalin, as compared with the stability of that from trans decalin has led us to postulate [4, 5] previously that the latter structure is the one representative of the solvent free gel system. The present observation of a transformation of the gel structure from cis decalin to that characterising gels from trans decalin strongly supports the contention that the latter structure is the more intrinsic (the difficulties in the interpretation of the layer line intensities notwithstanding).

#### Anomalous orientation effects

A further X-ray diffraction effect of potential interest was noted in the course of heat annealing *i*-PS gels formed from trans decalin. It was observed that provided the sample was held at fixed length during the heat treatment, the newly formed  $3_1$  helical structure appeared in two mutually perpendicular orientations. Figure 7 shows an example of a sample annealed at 120 °C, with only the  $3_1$  structure present and displaying this double orthogonal orientation. In

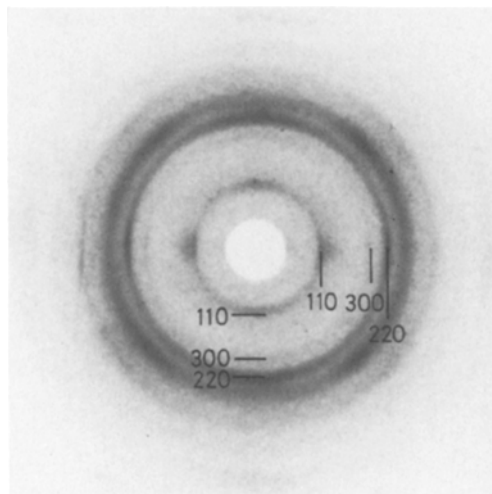


Fig. 7. X-ray fibre diffraction pattern of *i*-PS trans-decalin with sample held at fixed length during heat annealing at 120 °C. Two mutually perpendicular orientations of the  $3_1$  helix structure appear

figure 8 the sample was annealed at 100 °C which still contains some of the gel structure apparent by the presence of a diffraction arc at 0.51 nm on the meridian. (Note the relative strength of this diffraction signal compared to that in figure 2 for a 70 °C annealed sample underlining what we said about variability of  $3_1$  helix and gel structure ratios in the temperature regime where they may coexist). The double orthogonal orientation of the  $3_1$  helix structure is best apparent when inspecting the innermost 110 ring which reveals maxima both on the equator (as usual) and on the meridian. The same is apparent from the 220 reflection. Where the gel structure is simultaneously present this is in the usual parallel chain orientation as apparent from the meridional position of the 0.51 nm reflection (arrowed in fig. 8). It is seen from figure 8 that the 0.51 nm is distinct also through its straight line shape as opposed to the usual arc shape of the reflections corresponding to the  $3_1$  helical structure.

This distinction is significant as it demonstrates that the 0.51 nm diffraction signal of the gel structure is recognizably distinct from the  $hk0$  reflections of the  $3_1$  helix structure, and thus cannot be the consequence of a reflection from a closely similar spacing of the  $3_1$  helical structure present in some unsuspected orientation. This is being mentioned because such a situation has indeed arisen with drawn gels of PVC [13]. In the present case there can be no ambiguity: we have both the traditional  $3_1$  helix structure in two mutually perpendicular orientations and the new gel structure in its expected fibre alignment in the stretch direction.

The existence of two mutually orthogonal textures are also apparent from the two pairs of 211 reflections (arrowed) located close to the meridian and equator.

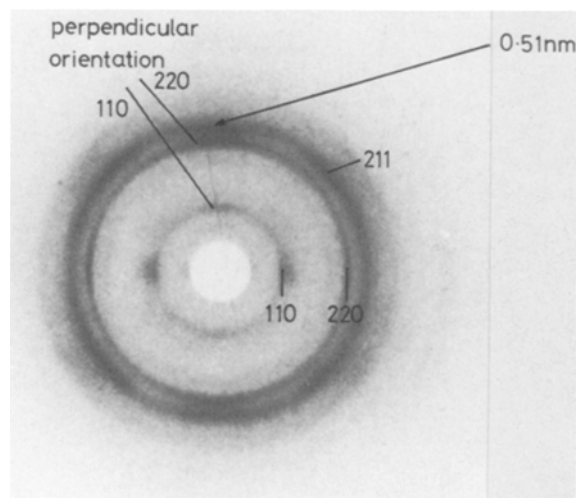


Fig. 8. X-ray fibre diffraction pattern of *i*-PS trans-decalin heat annealed at 100 °C with sample held at fixed length. Note in addition to the two mutually perpendicular orientations of the  $3_1$  helix structure; some gel pattern still persists by the presence of the 0.51 nm meridional diffraction signal (arrowed).

The detailed crystallography of this mutually perpendicular texture arrangement would deserve further discussion. Also the perpendicular orientation can have variants according to which lateral crystallographic axis of the orthogonal texture component aligns along the stretch direction, or whether there is any preferential lateral crystal direction axis at all (see review). All this will be treated in specific detail in a separate publication [1].

The interpretation of the morphological origin of perpendicular textures in oriented gels follows the lines laid out in our previous gel studies on other systems [1, 13]. It was envisaged that the orthogonal texture corresponds to platelet type crystals which are either unconnected or only loosely (i. e. not in a load bearing fashion) connected to the network. When the network is being stretched the junction forming crystals align with chain axis parallel to the draw direction which makes the crystal platelets, enmeshed within the network, align with the lamellar planes

<sup>1)</sup> We only mention here that the unusually sharp meridional reflection at 0.629 nm in figure 1 (arrowed) is attributable to the 300 reflection of the  $3_1$  helical structure in an orientation where the chains are perpendicular to the stretch direction, yet another manifestation of perpendicular orientation even if different in detail from the one in figures 7, 8. The recent identification of this reflection as one belonging to the  $3_1$  helix structure is highly welcome because this rather erratically appearing reflection was unaccountable on the basis of the gel structure and has thus been an anomaly so far, as just seen presently resolved.

parallel, hence with the chains perpendicular, to the stretching direction, thus producing the texture element responsible for the 'perpendicular' orientation. The identification of perpendicular textures in *i*-PS now provides a further strong support to this model. Namely, here we can clearly distinguish between the gel forming crystals by their different crystal structure and we see that these gel forming crystals are always in 'parallel' orientation. Or conversely, only the  $3_1$  helical structure gives rise to the 'perpendicular' orientation and we know that the platelet morphology is always associated with the  $3_1$  helical structure. Thus in the present case of *i*-PS the added distinction of morphology by crystal structure corroborates our previous ideas on the origin of the double orthogonal texture. Even so, this is not yet the full picture. The above morphological model refers to orientation of preexisting platelet crystals within the network. This would be certainly consistent with the observation of such orientation in unheated gels as in figure 1 (see footnote above), and indeed we have evidence (to be published) that the stretching of gels which were prepared deliberately so as to contain single crystals (turbid gels) show much enhanced perpendicular orientation in their  $3_1$  helical structure component. In figures 7, 8 however, the perpendicular orientation developed on heating, hence an additional factor involving oriented crystal growth needs invoking. It is likely that perpendicularly oriented platelet crystals present initially in small quantities, may develop further on heating in their initial orientation giving rise to the effect observed.

### Differential scanning calorimetry

Calorimetry was the first method by which these gels have been originally analysed and their melting and crystallization behaviour assessed; these were further extended in the present enquiry, in close association with the preceding X-ray and the following infra-red and electron microscope investigation. For a fuller appreciation some of the earlier results will be included in the account to follow.

It will be recalled [2] that the clear gel as formed reveals a sharp melting endotherm at  $\sim 60$  °C while the single crystal platelets in the appropriate suspensions show the same at  $\sim 120$  °C. The turbid gel containing both constituents show a double DSC peak at 60 °C (when the gel dissolves leaving behind a turbid suspension) and one at 120 °C when the suspension itself clears (fig. 9).



In subsequent stages of the investigation the gels were dried. Some of the work was done on oriented gels as such samples were used for the X-ray work. Presence or absence or orientation was of no consequence for the essential calorimetric features. The dry gels fall in two categories:

1) those which are only touch dry but may contain up to 20% solvent and

2) totally dry, obtainable, without destruction of the gel crystal structure, only by solvent extraction.

1) Examples of touch dry samples are represented by the thermograms of figure 10. The first feature to note is the small peak at  $\sim 60^\circ\text{C}$  (fig. 10a) during the original calorimetric scan. This peak disappears on prolonged heat annealing  $\geq 70^\circ\text{C}$  (fig. 10d) which while not explicitly assessed could well have expelled solvent. The peak also disappeared on solvent extraction as shown in figure 10g. This trace was obtained from a solvent extracted, completely dry, sample (without having a merely touch dry counterpart at that time). It follows from all this information that the small  $60^\circ\text{C}$  peak must be due to residual solvent in the touch dry sample in which part of the sample must apparently dissolve (melt) on heating. It evidently corresponds to the main gel peak in figure 9.

The next feature recorded when increasing the temperature is an endotherm  $\sim 99\text{--}114^\circ\text{C}$  and an

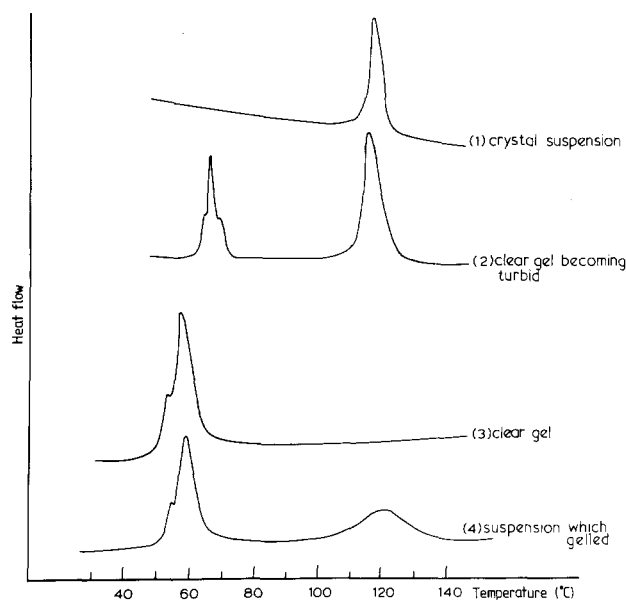


Fig. 9. DSC thermograms for *i*-PS gel, *i*-PS crystals and mixtures of the two forms. The clear gel as formed (curve 3) reveals a sharp melting endotherm at  $\sim 60^\circ\text{C}$  while the crystal suspension (curve 1) show the same at  $\sim 120^\circ\text{C}$ . The intermediate situations are shown in curves 2 and 4

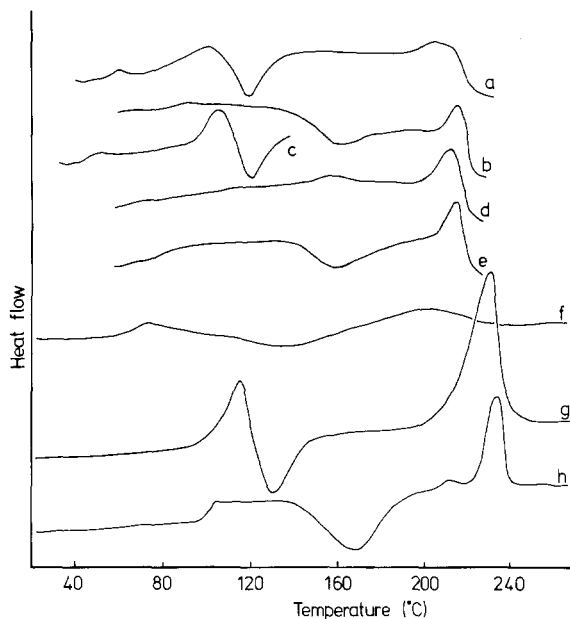


Fig. 10. DSC thermograms for *i*-PS samples heat annealed and treated in different ways.

(a) original calorimetric scan showing small peak at  $\sim 60^\circ\text{C}$

(b) rescan of sample (a) after cooling from  $220^\circ\text{C}$

(c) sample annealed at  $70^\circ\text{C}$  for 24h

(d) sample annealed at  $70^\circ\text{C}$  for 24h; followed by 0.5h at  $140^\circ\text{C}$

(e) rescan of sample (d)

(f) as-formed *i*-PS gel

(g) solvent extracted gel

(h) rescan of (g)

exotherm  $\sim 119\text{--}125^\circ\text{C}$ . This very characteristic endotherm – exotherm (apparent in figs. 10a, c, g) has been reported previously [5, 14] and is characteristic of the dry gel sample. The endotherm corresponds to melting and the exotherm to recrystallization, the former being associated with the disappearance of the gel structure and the latter with the formation of  $3_1$  structure as already foreshadowed by the preceding X-ray diffraction section and to be substantiated from the Fourier transform infra-red evidence to follow. As apparent from figure 10c annealing below the endotherm sharpens up this feature of the thermogram.

A prominent feature is the endotherm at  $213\text{--}235^\circ\text{C}$ . This corresponds to the melting of the dry  $3_1$  structure and clearly is the dried version of the  $120^\circ\text{C}$  dissolution peak obtained in the single crystal containing suspension (fig. 9). This peak has often featured in past literature and bears all the marks of the usual chain folded crystals, e.g. they shift to higher temperatures with heat treatment (above the gel melting region) they may appear as doublets or multiplets usually associated with refolding during a heating run or due to deliberate heat treatments. In

what follows we shall not be concerned with the behaviour of this endotherm any further beyond stating one important fact. Namely, that isotactic polystyrene normally crystallizes very slowly, requiring holding times of several hours even at the temperatures where the crystallization rate is maximum (170–180 °C). It is this crystallization which conventionally produces endotherms at ~220 °C. In our case such crystallization must have occurred during the heating up process in the DSC and this must have been confined to within the scanning time which at our heating rate of 10 °C/min could not total more than 20–25 minutes. If we now consider that the sample could have spent only a fraction of this period, hence a few minutes, in the temperature interval where crystallization is likely to occur, it follows that the crystallization producing the 220 °C endotherm must have become greatly accelerated. Clearly this must be due to the initial gel consistency and the underlying gel structure which thus must promote crystallization even in the normal ( $3_1$  helix) form even after the gel has melted by the present DSC and preceding X-ray diffraction criterion. What is more, the ~220 °C appears even after a rerun of the sample after cooling from temperatures above 220 °C (figs. 10b, e, h) indicating the persistence of some crystallization memory. All these accelerated crystallization effects are rather remarkable and could be significant for the potential practical application of *i*-PS. This effect, first recognized by DSC, will recur again in the infra-red and electron microscope section where it will be taken further.

A few remarks will be made on what can be observed in between the 99–125 °C endotherm-exotherm pair and the final melting peak at ~220 °C. During a straight first run on the dried gel there are no detectable features in the thermogram in this intermediate region [5]. On a rerun, after complete melting to room temperature (under conditions where the accelerated crystallization holds) there is an exotherm at around 150–180 °C (figs. 10b, e, f). In a series of experiments the initial gel samples were annealed at different temperatures. As already stated annealing below the 105 °C peak preserved, in fact sharpened the gel endotherm (fig. 10c). Annealing above the 99–125 °C endotherm-exotherm pair indeed removed this pair (fig. 10d), indicating amongst others that the gel structure has melted out irreversibly. In addition a new feature appears as a result of such an annealing treatment: a small but distinct endotherm at 150–160 °C moving to higher temperatures up to 180 °C with increasing annealing temperature. It remains distinct from the main endotherm in the 230 °C

range which also sharpened and moves to slightly higher temperatures as a result of such annealing. This small endotherm in the 150–180 °C region appears only on the first annealing of the initial gel structure. Rerunning of the fully molten sample gives the first mentioned exotherm at around 150–180 °C (and not the endotherm) irrespective of the preceding thermal history. The full evaluation of what is happening is clearly being called for. Material in an accompanying paper specifically devoted to the accelerated crystallization will throw at least some light on it. The first question which arises phenomenologically concerns the possible relation between the different exotherms and endotherms. However, this will not be pursued here<sup>2</sup>). The present section of DSC serves mainly to bracket by calorimetry the existence regimes of the different crystal forms and their transformation in service of the morphological studies to follow further below.

### Infra-red spectroscopic study of the gel crystals

That the gel structure has fingerprints in the infra-red spectrum has been noticed previously [2, 17]. Also some still earlier infra-red observation by Kobayashi et al. [15] have been shown to be due to gel formation [16] even if not recognized as such at the time. The same early works also identified the usual  $3_1$  crystals by their spectroscopic fingerprints which were distinct from those due to the gel crystals. All these early works were much handicapped by the overlaying solvent spectrum. The advent of the Fourier transform methods with its subtraction capabilities greatly promoted this line of work.

This was utilized by Painter et al. [12] in their more recent study of *i*-PS gels as to be detailed below. In the present work we now exploited the improved capabilities of the infra-red technique in service of the issues covered by this paper. These are: compare gels from trans and cis decalin, follow the changes in the

<sup>2</sup>) Such questions are e.g.: does the exotherm at ~120 °C correspond quantitatively to the endotherm at ~105 °C, namely to the recrystallization of the gel material which has just melted? Reference [14] claims that this is so. Inspection of the traces indeed suggests this, as the exotherm seems closely an inverted form of the preceding endotherm. Nevertheless we have evidence that this cannot be the whole story as some of the gel structure survives the temperature range of the exotherm as in fact apparent from the infra-red analysis to follow. As far as the exotherm area is truly equivalent to that of the endotherm this would necessarily imply that material contributing from the endotherm cannot all come from the gel crystals. Clearly more detailed and critical evaluation of this point is required.

gel structure on heating and the appearance of the  $3_1$  helical structure during the process, together with the noting of the orientation effects through dichroism. In the next section we shall use these results further in aid of the assessment of the effect of drying. Even if the various bands to be referred to are not all fully assigned, they serve as fingerprints of the relevant structures. Without any further rigour the significance of the effects lies in the fact they reflect differences in chain conformation associated with the different structures.

Painter et al. [12] has identified a range of bands associated with the gel of *i*-PS within the infra-red spectrum. In particular, gel bands appear at  $1061\text{ cm}^{-1}$ ,  $1069\text{ cm}^{-1}$ ,  $916\text{ cm}^{-1}$  and  $894\text{ cm}^{-1}$ . The latter pair relate to the  $922\text{ cm}^{-1}$  and  $899\text{ cm}^{-1}$  bands characteristic of the  $3_1$  helical structure [16] but are shifted to lower frequency presumably as a result of the greater restrictions imposed by interactions between the aromatic groups of contiguous units in the extended structure. Observations of the intensities of these gel bands relative to the bands from the amorphous *i*-PS allows us to follow the melting of the gel crystallites. In addition, a new 'gel' band has been observed at  $562\text{ cm}^{-1}$  which again may be related as above to the  $566\text{ cm}^{-1}$  band characteristic of the  $3_1$  helical structure. (This spectral region while studied will not be illustrated). The samples chosen were oriented gels formed from trans and cis decalin, they were touch dried (such as the sample in fig. 10a used for the DSC), i. e. should contain up to 20% solvents, the spectra of the latter having been appropriately subtracted. The spectra were taken with both parallel and perpendicular polarization.

The spectra were recorded with unpolarised light and with polarised light, in the latter case both with the polariser parallel and perpendicular to the draw direction. The latter was done in the first instance because the relevant bands showed up more clearly in one or the other direction of polarization and of course because the dichroic effects provide information on orientation.

#### *i*-PS trans decalin gel

This sample was annealed at 60, 75, 90, 120 and  $150^\circ\text{C}$ . The infra-red spectra of the unannealed gel shows the presence of a very small amount of  $3_1$  helix structure (i. e. bands at  $922\text{ cm}^{-1}$  and  $566\text{ cm}^{-1}$ ), but are dominated by the gel bands. The polarized spectra for the unannealed gel are shown in figure 11 for the  $1400$  to  $800\text{ cm}^{-1}$  region. The important gel bands in this region are indicated.

After annealing at  $150^\circ\text{C}$  the polarized spectra are dominated by bands characteristic of the  $3_1$  helix structure, as illustrated in figure 12. In particular, the  $3_1$  helix bands at  $899$ ,  $922$  and  $982\text{ cm}^{-1}$  are indicated, to show some of the important spectral differences between figures 11 and 12. The absence of bands at  $1069$  and  $1061\text{ cm}^{-1}$  may also be seen. Also many further differences between the spectra in figures 11 and 12 may be observed, not to be commented on individually at this place. There are differences in relative intensities of bands as well as slight shifts in positions of bands. Although these differences are not as obvious as those in the region of  $900\text{ cm}^{-1}$  and the  $1100$  to  $1050\text{ cm}^{-1}$  region, they can still be used as an indication of the state of the sample.

The spectra obtained from the sample annealed at the temperatures between room temperature and  $150^\circ\text{C}$  indicate how the transition from the gel structure to the  $3_1$  helix structure occurs with increasing temperature. Annealing at temperatures below  $100^\circ\text{C}$  produces a lowering of the intensity of the gel bands, but there is no accompanying increase in intensity of the  $3_1$  helix bands. Annealing at  $120^\circ\text{C}$ , however, produces a significant change in the spectra, the gel bands are almost completely removed from the spectra but not quite (there are still signs of the  $916\text{ cm}^{-1}$  and  $562\text{ cm}^{-1}$  gel bands), and at the same time the intensity of the  $3_1$  helix bands is greatly

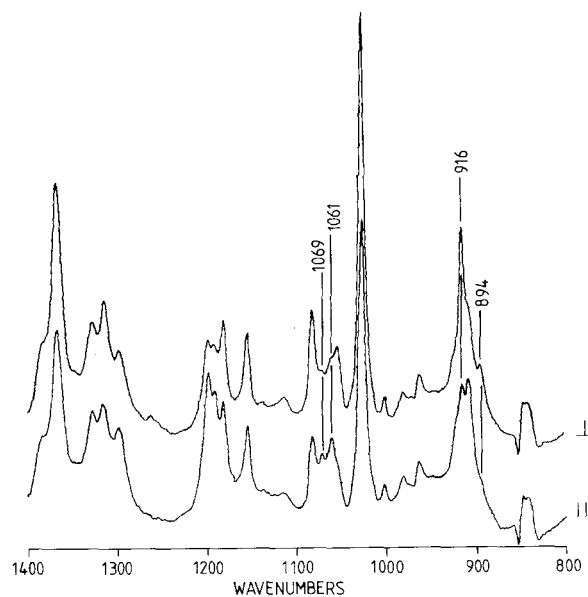


Fig. 11. Polarized spectra in the region  $1400$  to  $800\text{ cm}^{-1}$  for an unannealed *i*-PS trans-decalin gel after spectral subtraction of solvent

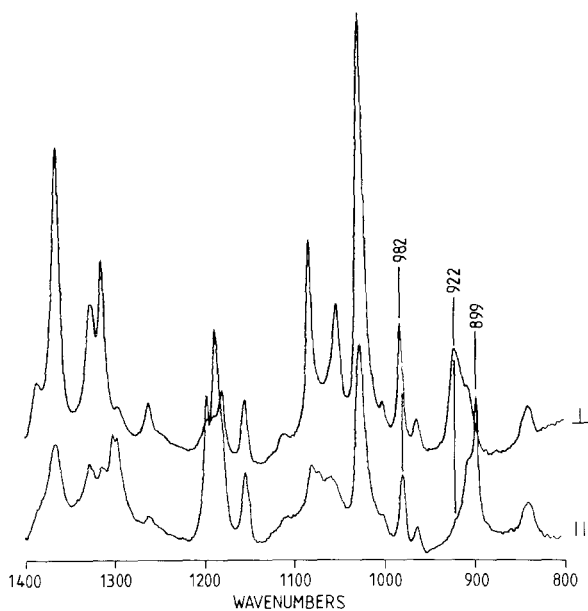


Fig. 12. Polarized spectra in the region  $1400$  to  $800\text{ cm}^{-1}$  for an *i*-PS trans-decalin gel after annealing at  $150\text{ }^{\circ}\text{C}$

increased. Further annealing at  $150\text{ }^{\circ}\text{C}$  produces a small increase in  $3_1$  helix structure.

The spectra in the region of  $900\text{ cm}^{-1}$  which most clearly illustrate the annealing behaviour are shown separately for a full sequence of annealing temperatures (fig. 13) between the two end states represented

by figures 11 and 12 displaying several stages of the transformation of the gel structure to that of the  $3_1$  helical structure with a small residual gel remaining. As in figures 11–12 this is again shown for two polarization directions.

#### *i*-PS cis decalin gel

This sample was annealed at  $45$ ,  $69$ ,  $90$ ,  $120$  and  $150\text{ }^{\circ}\text{C}$ . The polarized spectra for the unannealed gel and for the gel annealed at  $150\text{ }^{\circ}\text{C}$  are identical to those for the *i*-PS trans decalin gel, except that here the spectra of the unannealed gel show no sign of the  $3_1$  helix structure.

Annealing above room temperature reduces the gel component, and in this case an annealing temperature of only  $60\text{ }^{\circ}\text{C}$  almost completely removed the gel bands from the spectra and at the same time the first trace of the  $3_1$  helix structure could already be detected. Increasing the annealing temperature to  $90\text{ }^{\circ}\text{C}$  produced a large increase in intensity of the  $3_1$  helix bands, and there was hardly any sign of the crystalline gel component. Further annealing at temperatures above  $90\text{ }^{\circ}\text{C}$  showed only a small increase in the amount of  $3_1$  helix structure. Figure 14 is a parallel to figure 13 showing the set of polarized spectra obtained for the *i*-PS cis decalin gel for a range of

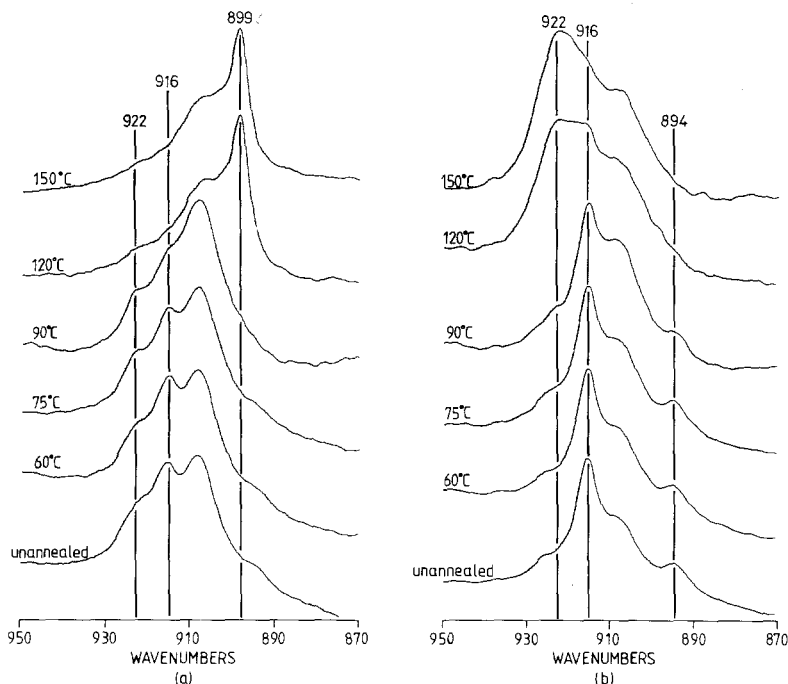


Fig. 13. Annealing series of spectra for *i*-PS trans-decalin gel in the region  $950$  to  $870\text{ cm}^{-1}$ : (a)  $\parallel$  spectra; (b)  $\perp$  spectra

annealing temperatures, for the conformationally sensitive region of  $900\text{ cm}^{-1}$ .

The principal conclusions emerging from the infra-red studies are:

i) In accordance with Painter et al. [12] and the earlier works the gel structure displays distinct spectral features.

ii) There is no difference in the infra-red spectra prepared from trans and cis decalin (in spite of differences of the X-ray spectra).

iii) The infra-red spectra confirm the melting of the gel and appearance of the  $3_1$  helical structure on heating. The pattern of changes on heating is broadly the same as observed by X-ray diffraction and DSC, although there are some additional effects. One of them is the persistence of the last traces of the gel up to  $150^\circ\text{C}$  (in the preparation from trans decalin), information which will acquire significance further below.

iv) The orientation of both structures is confirmed by the dichroic effects. The high degree of orientation of the  $3_1$  helical structure is specially noticeable, and particularly notable is the fact that the  $3_1$  helical structure forms in an oriented state. We have quantified these dichroic effects but as these data do not contribute to the issues in the present paper the subject will not be pursued here further.

### Infra-red investigation on the effect of solvent

The effect solvent may have on the gel structure has been an issue ever since the first observations. It has been highlighted by the recent articles by Sundararajan [10, 11] who claimed that a substantial amount of solvent is in fact necessary for the existence of the gel structure which becomes incorporated in this structure thus stabilizing it. As this issue is clearly fundamental for the whole topic and affects the continued pursuance of it we gave it special attention.

It was stated previously [3, 5] that the usual dried trans decalin gel sample contained 18–20% and the dried cis decalin sample about 26% of solvent, even if the sample appeared dry to the touch. Attempts to extract this solvent indeed destroyed the gel structure from cis decalin producing a conversion into the  $3_1$  helical structure, indicating that solvent is indeed necessary for this structure to exist. However, the structure from trans decalin could be preserved even on complete drying as testified by DSC calorimetry and more specifically by X-ray diffraction [5], the DSC effects being reproduced here (fig. 10g) and the X-ray effect mentioned earlier in the present paper. The sum total of these effects have been interpreted by maintaining that the extended type chain conforma-

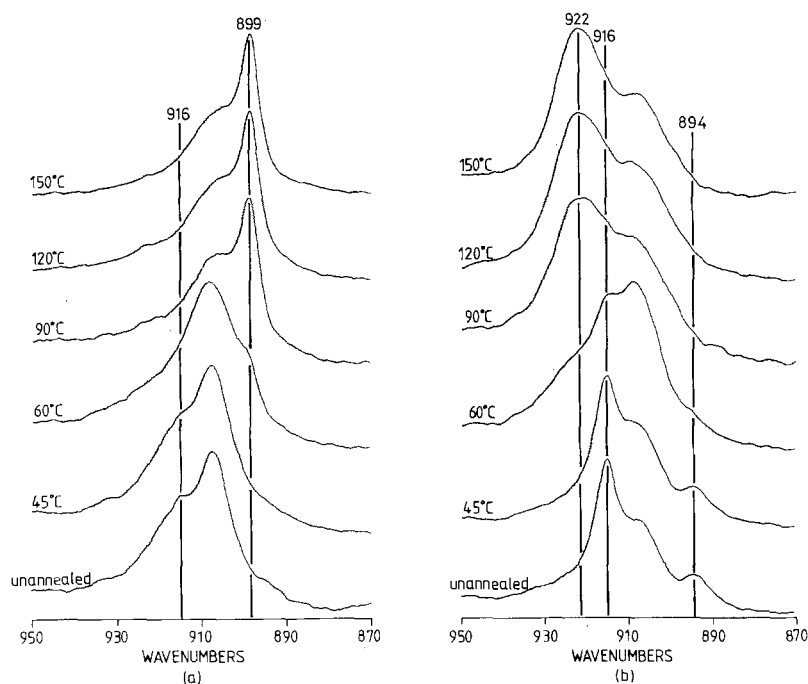


Fig. 14. Annealing series of spectra for *i*-PS cis-decalin gel in the region  $950$  to  $870\text{ cm}^{-1}$ : (a) // spectra; (b)  $\perp$  spectra

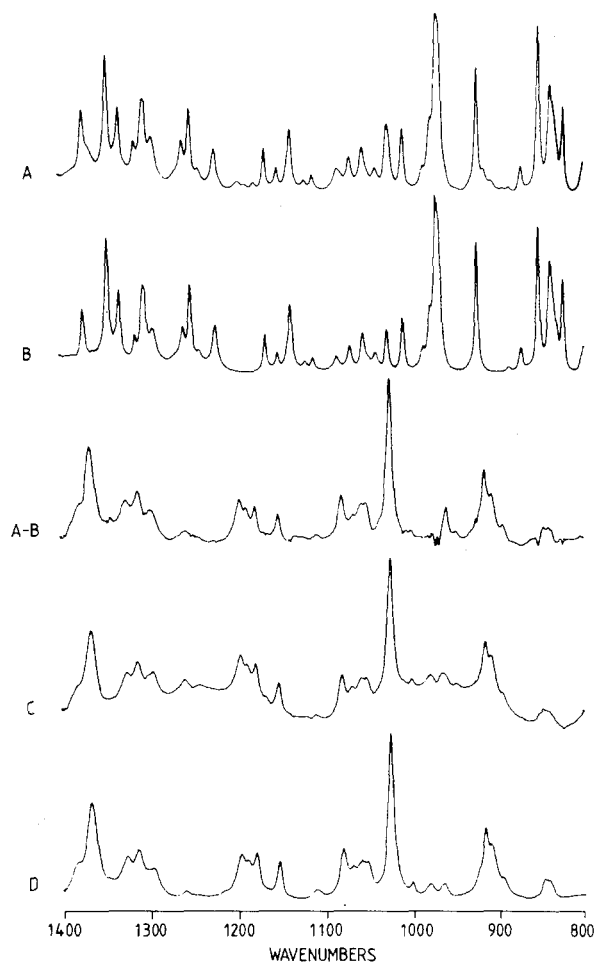


Fig. 15. (A) Spectrum of *i*-PS trans-decalin gel in the wet state (5% polymer concentration). (B) Spectrum of trans-decalin. (A-B) Spectrum of *i*-PS in the wet gel, obtained by subtracting the trans-decalin spectrum from the gel spectrum. (C) Spectrum of *i*-PS in the touch dry gel after residual solvent bands have been subtracted. (D) Spectrum of *i*-PS after extraction of solvent from the gel

tion can be stable *without* any solvent, its manifestation being the gel structure as obtained from trans decalin while the gel structure from cis decalin is a modification of it, not as regards chain conformation but chain packing, stabilized by occluded solvent. Thus while admittedly the gel structure can be modified by occluded solvent (and in fact is prone to occlude solvent) it does not rely on the solvent for its existence.

Clearly the above conclusion is contrary to that at Sundararajan and consequently its validity acquires added significance and also requires further scrutiny. In particular, the notion of absence of solvent needs explicit quantification. This was now undertaken by

using infra-red spectroscopy to assess the amount of residual solvent through the spectrum of the solvent itself. At the same time the subtraction capability of the FTIR also enabled us to follow the effect of drying on the spectrum of the polymer. This investigation on the effect of drying from both viewpoints, will be briefly reported.

Two stages of drying were considered:

i) The first concerns the change in solvent concentration when a gel is allowed to dry in air until touch dry. ii) The second concerns the removal of residual solvent present in this touch dry state.

i) A film of *i*-PS trans decalin gel was prepared, having a polymer concentration of 5%. The infra-red spectrum of the gel in this wet state was recorded. The sample was allowed to dry in air for several days until touch dry, and the infra-red spectrum was again recorded. Comparison of the relative absorbances of the  $560\text{ cm}^{-1}$  polymer band and the  $600\text{ cm}^{-1}$  solvent band in both the wet and touch dry states revealed that in the touch dry state the sample contained 17% solvent. The spectral subtraction capability of the FTIR spectrometer was used to 'remove' solvent and reveal the polymer spectrum in both the above states. In figure 15 the subtraction of solvent from the spectrum of the wet state is shown and the resulting polymer spectrum is compared with the *solvent subtracted* spectrum of the gel in the touch dry state. It can be seen that the spectrum, and therefore the polymer conformation is unchanged.

ii) As a next step an attempt was made to completely extract the solvent experimentally. A touch dry gel was placed in acetone for 24 hours in order to exchange the solvent. The sample was then dried under vacuum. The infra-red spectrum of the gel after this extraction procedure is compared in figure 15D with the solvent subtracted spectrum of the touch dry gel. Again we find that the spectrum, and therefore the polymer conformation, is unchanged. Also there is no obvious sign of solvent bands in the spectrum of the extracted gel. Closer analysis reveals that solvent, if present, must be in a concentration of less than 0.4%.

In summary, we note that the 'fully dried' sample is truly solvent free within the limits stated. The amount of solvent which could perhaps be accommodated within the above error limits would be certainly insufficient to be responsible for the stabilization of the near extended chain conformation, in the sense envisaged by Sundararajan. Further, we note that the nature of the gel structure remains unaffected throughout solvent removal, i. e. over a polymer concentration range of 5% to 100%. In addition as seen from figures 15 (A-B), (C) and (D) not only the

nature of the spectrum but also the intensity is unaffected over the full spectral range recorded (the spectra are from the same amount of material recorded with the same sensitivity) an impression confirmed by quantitative assessment. Thus not only the nature of the gel but even its amount remains unaffected by drying, i. e. no further gel forms as the solvent is removed. This is very significant because it ensures that the study of the dried gel provides a representative assessment of the gel in situ.

All the preceding methods serve to provide an assessment of the crystal constituents of the gel preparations by macroscopic properties (DSC) by crystallographic evidence (X-ray diffraction and by chain conformation), infra-red spectroscopy, even if applied here only in a finger printing manner. Clearly we also want to have information on the underlying morphologies. Such information was provided in the first instance by X-ray diffraction (other than that relating to the crystal structure) which, as we shall see, has led to some explicit inferences to be reported in the next section. These as will be apparent, have led to certain anticipations which become strikingly confirmed by electron microscopy, the final and principal section of this paper.

## Crystal size – morphology by X-ray diffraction

### *X-ray diffraction line width*

It is conspicuous by inspection that the 0.51 nm diffraction signal in the gel structure is narrow and that the 102 reflection in the  $3_1$  helix structure is broad. This difference is most strikingly apparent in diffraction patterns containing both structure patterns simultaneously such as in figures 3, 4. As the 0.51 nm signal is on the meridian and the 102 reflection closely so, both correspond to periodicities exactly or (in the case of the 102 of the  $3_1$  helix structure) closely along the chain direction. The above observation therefore must mean that crystals in the gel structure are long in comparison to those in the  $3_1$  helix structure. This point was commented on previously [2] associating the two features with fibrillar and lamellar morphologies respectively, also assigning rough values to the crystal sizes along the chain direction ( $\sim 20$  and  $\sim 10$  monomer units in the gel and  $3_1$  helical structure respectively). Presently, however, we are anxious to reemphasize this fact in a somewhat different context. Namely in figures 2, 3, the  $3_1$  helix structure arose through heating following the melting of the gel structure. One would therefore expect the  $3_1$  helix structure to be the stabler one of the two which the

system is trying to achieve, a fact indeed borne out by its much higher melting point. Nevertheless at this point a paradox arises, namely that the stabler crystals are smaller along the fibre direction (the physically most important direction as it corresponds to that of the polymer chains) than the less stable crystalline form. This fact on its own indicates that we are not dealing with a simple transformation from one structure to another on heating, as it would be totally unaccountable why such a transformation should lead to a significant reduction in crystal size. The importance of this point will be borne out by the electron microscopy later. The sharpness of the equatorial reflections corresponding to the  $3_1$  helical structure may be remarked in passing: it reflects the well developed lateral size of the coherently diffracting crystal compared with its size along the chain direction.

### *Low angle X-ray diffraction*

With the above morphological implications in mind the various samples were examined for low angle X-ray diffraction.

The oriented gel structure showed no discrete reflection only a diffuse scatter around the central beam (fig. 16). However, on heat annealing a very characteristic meridional diffraction peak develops. Figure 16 shows the full series. We see that with our sampling the first indication of the discrete diffraction peak appears at a spacing of  $13 \pm 1$  nm and at an annealing temperature of  $75^\circ\text{C}$ , it becomes pronounced for annealing temperatures of  $107^\circ\text{C}$  with the spacings changing to  $11.7 \pm 1$  nm. Annealing at  $150^\circ\text{C}$  the diffraction spots become even more pronounced, although the spacing remains constant, and by which time much of the continuous scatter has disappeared. Clearly the appearance of this discrete low angle peak is associated with the disappearance of the gel and the development of the  $3_1$  helical structure.

The most conspicuous features of the discrete low angle peak are as follows: i) its high intensity; ii) in spite of i) it never displays higher orders, invariably only one order is present; iii) it has a characteristic round shape revealing no spread either along a layer line nor any arcing around a circle.

i) means clearly that the peak must correspond to a significant structural feature which is both representative and is associated with a large fluctuation in electron density.

ii) must mean that the underlying periodicity, or at least its projection on the fibre direction, is poorly developed.

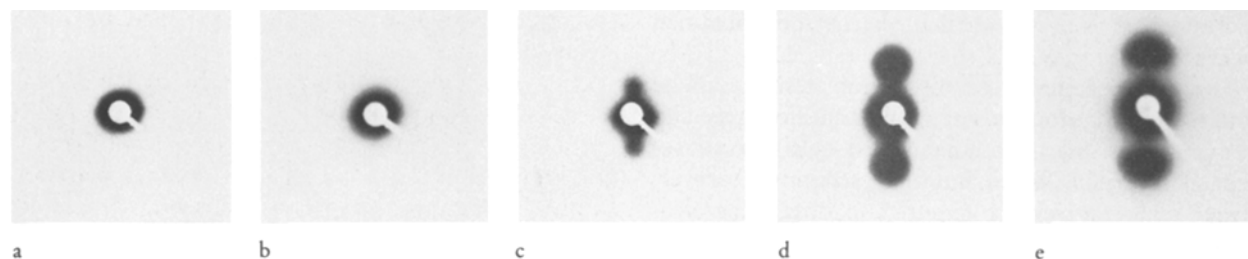


Fig. 16. Low angle X-ray diffraction patterns obtained from *i*-PS trans-decalin gels after heat annealing at various temperatures (a) 20 °C, (b) 45 °C. A discrete diffraction peak appears at 75 °C (c) and becomes pronounced on annealing at 107 °C (d) and even more so for 150 °C (e)

For iii) we have no a priori explanation except for an empirical analogy. Namely, this kind of diffraction signal now seen, has in the past always been associated with shish-kebab or row nucleated type structures. In fact the appearance of such diffraction patterns was always an infallible indication of the existence of such structures (e. g. ref. [18]). It is with expectations arising from this analogy that the electronmicroscopic examination, to be described in what follows, was undertaken.

## Electron microscopy

### Electron diffraction

Electron diffraction patterns from unannealed and fully annealed *i*-PS samples (originally cast from trans decalin) are seen in figures 17a and 17b. The unannealed samples show the characteristic 0.51 nm meridional diffraction signal (fig. 17a). The fully annealed samples show the full  $3_1$  helix fibre pattern (fig. 17b). Samples annealed at intermediate temperatures (80–100 °C, annealing in the bulk) showed gel pattern from some selected areas and  $3_1$  helix pattern from others. The  $3_1$  helix diffraction pattern predominated as the annealing temperature was raised. Samples from trans decalin annealed in the bulk at 120 °C show  $3_1$  helix structure only. These findings agree with those obtained by the other-techniques.

The changes in diffraction pattern were observed with time as samples were annealed at constant temperature in the electron microscope. On annealing at 124 °C, it was found that the gel diffraction pattern faded and vanished, to be replaced by an amorphous halo, in the first 3 minutes. On holding the sample at 124 °C for a further period, the  $3_1$  helix pattern appeared and gradually strengthened over a period of about 2 hours. The gel and  $3_1$  helix patterns were not observed together. It was occasionally possible to

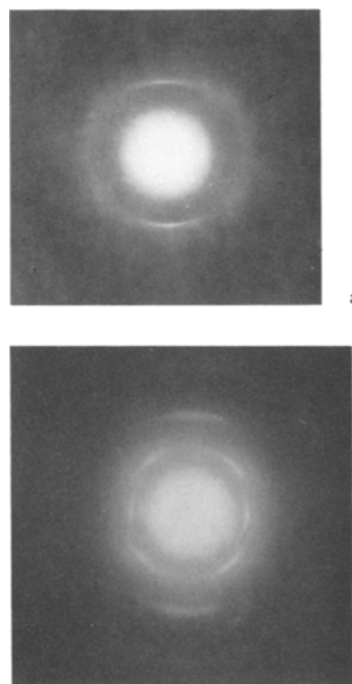


Fig. 17. (a) Electron diffraction pattern of a longitudinal section of an oriented, unannealed *i*-PS gel prepared from trans-decalin (b) Electron diffraction pattern of a longitudinal section cut from an oriented *i*-PS gel prepared from trans-decalin and annealed for 1 day at 150 °C before sectioning.

obtain a superposition of the two patterns from large selected areas of samples annealed at intermediate temperatures (as it was from X-ray samples); when the selected area was reduced to the order  $1/\mu\text{m}^2$  the regions of sample giving rise to each pattern could be separated and were seen to have different morphologies. This electron diffraction study indicates that the gel crystals melt, or at least cease to diffract, before the  $3_1$  helix crystals are formed. On a square



micron scale the two structures are not obtained together.

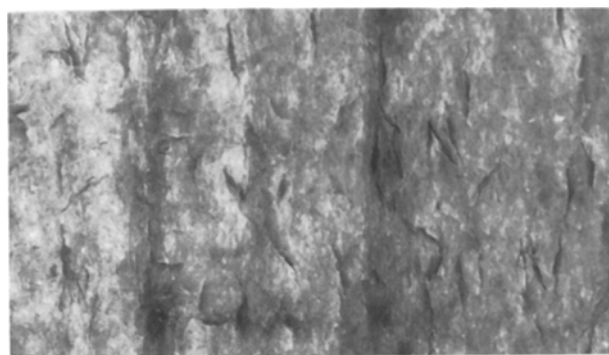
The same sequence of diffraction results can be obtained from samples cut from annealed gels and from samples cut from unannealed gels and subsequently annealed. When annealing sections, however, higher temperatures are required to obtain the electron diffraction equivalent of the X-ray diffraction fingerprint. A gel pattern only is observed from a section cut from unannealed material and subsequently annealed at 80 °C. The highest temperature of annealing in the bulk to retain a gel pattern alone is 65–70 °C.

No diffraction patterns were ever obtained from unannealed samples cast from *cis* decalin. Methods of low temperature sectioning and electron microscopy were attempted, but a diffraction pattern was still unobtainable. However, when a gel from *cis* decalin had been annealed to 45 °C previous to sectioning, a diffraction pattern was obtained from sections, a pattern similar to that given by *trans* decalin gel sections (fig. 17 a). This last finding is in agreement with the X-ray results.

This unobtainability of the *cis* decalin gel diffraction pattern may be a consequence of the need for solvent to remain in the gel for the characteristic *cis* decalin gel diffraction pattern to be retained. It is possible that the vacuum of the electron microscope removes all remaining *cis* decalin and the gel no longer diffracts. On the other hand the *trans* decalin gel continues to diffract without solvent.

### Morphology

The striking change in electron diffraction pattern is accompanied by a corresponding change in morphology observed in longitudinal sections seen in the transmission electron microscope. Figure 18a shows a typical view of the unannealed material. It consists of an essentially featureless background with, what appears, as a few thick wrinkles parallel to the stretch direction. On annealing to 60° the diffraction pattern remains unaltered (as fig. 17a) but the morphology becomes more open and fibrous (fig. 18b), with many small fibres running in the fibre direction of the diffraction pattern. On annealing a sample such as that in figure 18a to 90–120 °C while in the electron microscope, lamellae are seen to grow at right angles to the fibre direction. Growth can be followed over a period of several hours (although not growth of the same crystals since the electron beam 'freezes in' the structure on irradiation). Figure 18 c shows an area after crystallization for some hours at 90° and fig.



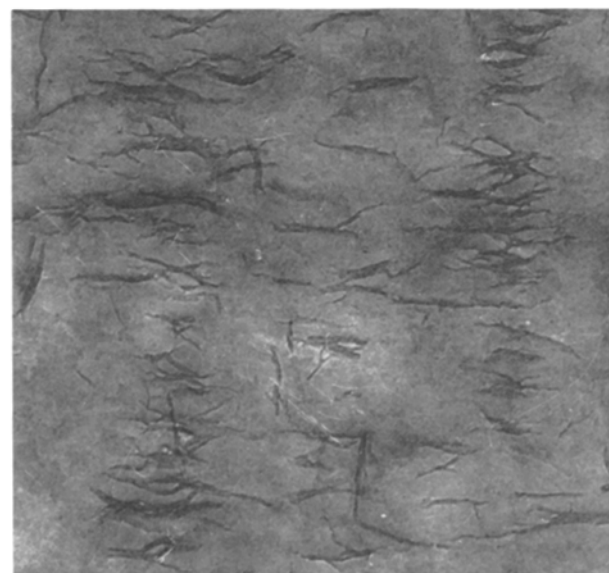
×60K

a



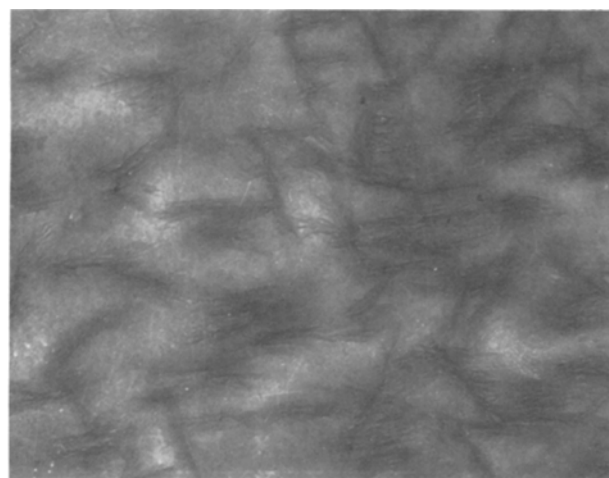
×60K

b

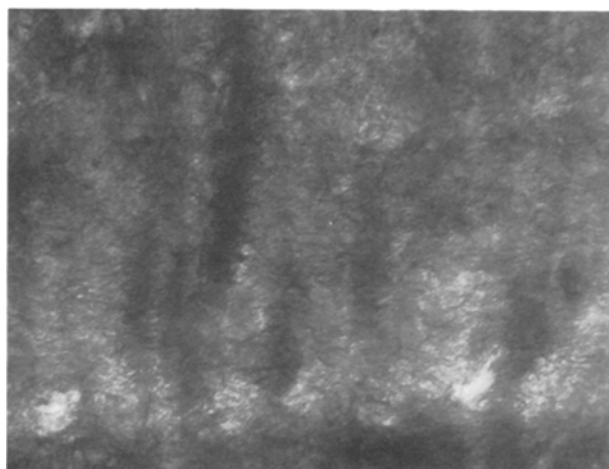


×60K

c



d



e

Fig. 18. (a) Transmission electron micrograph of a longitudinal section cut from an oriented, unannealed *i*-PS gel prepared from trans-decalin. The section was extracted with acetone for 2 hrs. Magnification sixty thousand (draw direction vertical in each case). (b) Transmission electron micrograph of a longitudinal section cut from an oriented *i*-PS gel, prepared from trans-decalin and annealed for 1 day at 60 °C previous to sectioning. The section was extracted with acetone for 1 hr. Magnification sixty thousand (c) Transmission electron micrograph of a longitudinal section cut from an oriented, unannealed *i*-PS gel prepared from trans-decalin and annealed overnight at 90 °C after sectioning. Magnification sixty thousand (d) Transmission electron micrograph of a longitudinal section cut from an oriented gel prepared from trans-decalin and annealed overnight at 150 °C after sectioning. Magnification sixty thousand (e) Transmission electron micrograph of a longitudinal section cut from an oriented gel prepared from trans-decalin and annealed for 1 day at 150 °C while stressed before sectioning. Section extracted with acetone for 2 hrs. Magnification sixty thousand

18 d. shows an area after crystallization at 150 °C. This latter electron micrograph shows a characteristic 'double' or 'crossed' orientation which has a diffraction pattern of two  $3_1$  helix fibre patterns superimposed at right angles. Crossed fibre patterns have also been seen by X-ray diffraction of specially prepared samples (see X-ray section above (fig. 7)). The lamellae are seen to be quite far apart in annealed sections. Sections of samples annealed under stress in the bulk show much more closely spaced lamellae (fig. 18e). These lamellae appear undulating and are nucleated in columns, an effect previously noted in shish-kebab structures of polyethylene [18].

In transverse section, unannealed samples appear mottled and dotted on a 30–60 nm scale (fig. 19a). Transverse sections annealed for two hours at 120 °C in the electron microscope show circular or hexagonal crystals appearing (fig. 19b). Transverse sections of  $3_1$  helix samples prepared by annealing in the bulk previous to sectioning show densely packed crystals about 50 nm in diameter, many overlapping each other (because there are many crystal thicknesses within a section thickness). Individual crystal diffraction patterns were unobtainable,  $hk0$  rings (of the  $3_1$  helix) were always recorded.

### Dark field

The unannealed gel gives a characteristic electron diffraction pattern, similar to that obtained with X-rays. The corresponding morphology shows fibres running parallel to the fibre direction of the diffraction pattern. Dark field micrographs of these sections, using the 0.51 nm diffraction signal reveal rather isolated areas of intense diffraction with strings of diffracting units of 20–50 nm in length and about 10 nm in width. Several areas of the same sample are shown in figure 20a.

A dark field micrograph using the 102 reflection of a section of sample prepared from cis decalin and annealed, as a section, at 111 °C is seen in figure 20 b. A large number of lamellar crystals are seen lying at right angles to the fibre direction of the sample. In this material the lamellae are widely spaced and no 'shish-kebab cores' can be seen in the dark field micrograph. However, where samples were sectioned after annealing and the structure is much finer, cores can sometimes be seen linking the lamella crystals. Figure 20c is the bright field micrograph of the sample used to obtain figure 20b. It reveals that the region is in fact one of double orientation, but that only one set of lamellae was selected by the dark field microscopy

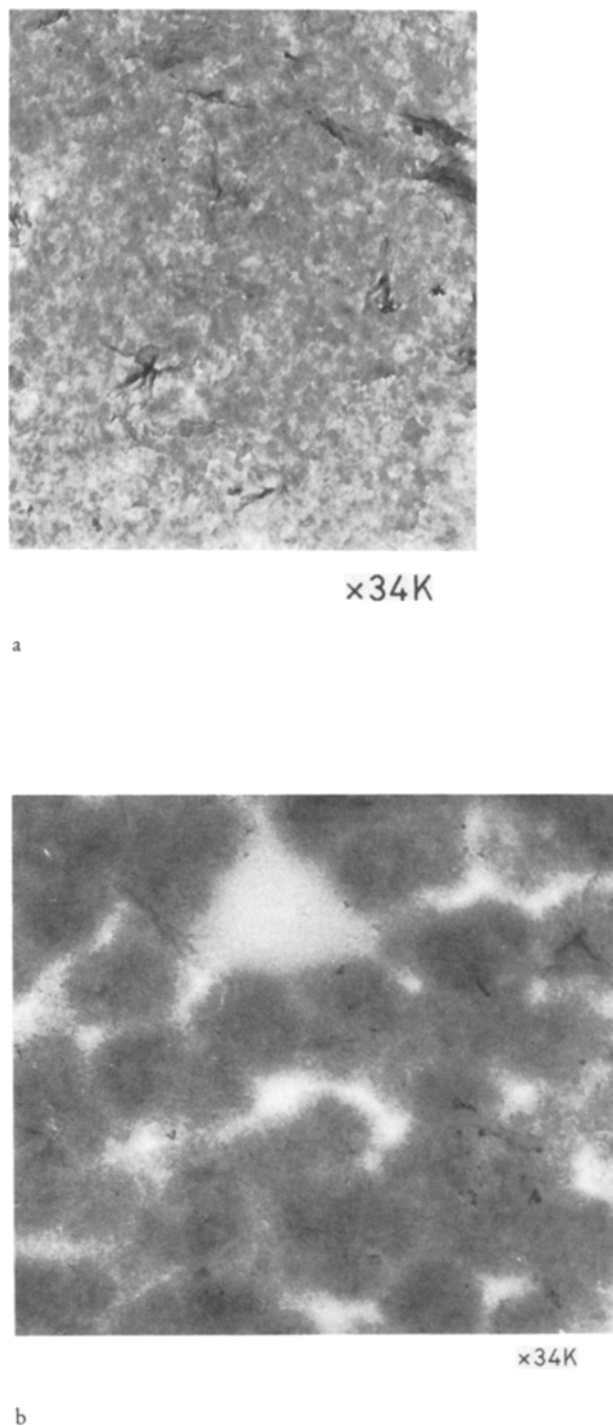


Fig. 19. (a) Transmission electron micrograph of a transverse section cut from an oriented, unannealed *i*-PS gel prepared from trans-decalin. Section extracted with acetone for 1 hr. Magnification thirty-four thousand

(b) Transmission electron micrograph of a transverse section prepared as in 19a, but without extraction. Instead the section was annealed at 120 °C in the electron microscope for 1.25 hrs after sectioning. Magnification thirty-four thousand

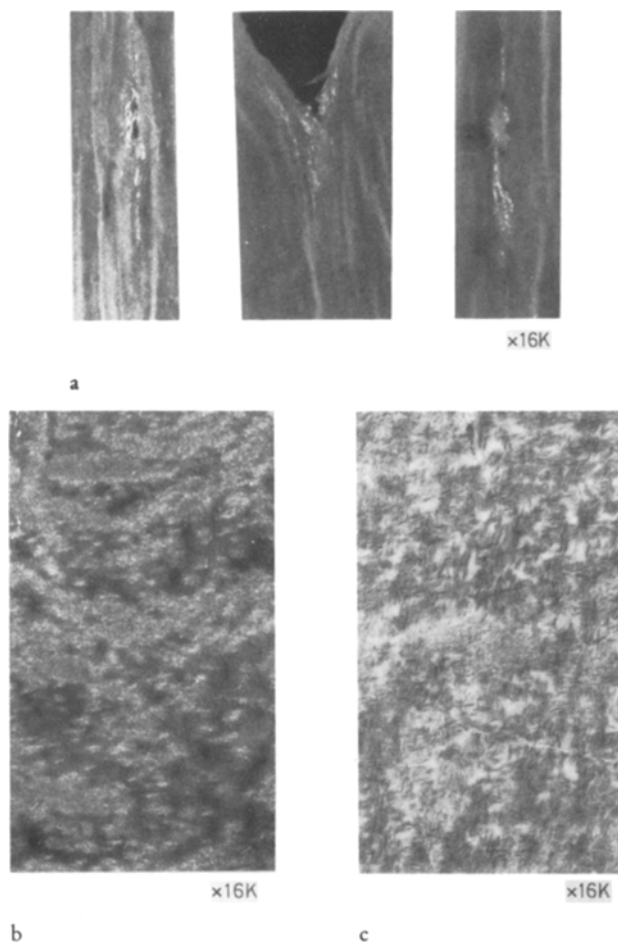


Fig. 20. (a) Dark field transmission electron micrographs (using the prominent 0.51 nm reflection) of a longitudinal section cut from unannealed, oriented *i*-PS gel, prepared from trans-decalin. Parts of the sample showed intense diffraction, much did not. It is thought that this may be due to thickness differences – the diffracting regions occur around cracks and holes. Magnification sixteen thousand

(b) Dark field transmission electron micrograph (using one 102 reflection) of a longitudinal section cut from unannealed, oriented *i*-PS gel prepared from cis-decalin and annealed as a section, at 111 °C for overnight. Magnification sixteen thousand

(c) Bright field transmission electron micrograph of the part of the section shown in dark field in figure 20b, revealing a crossed morphology. Magnification sixteen thousand

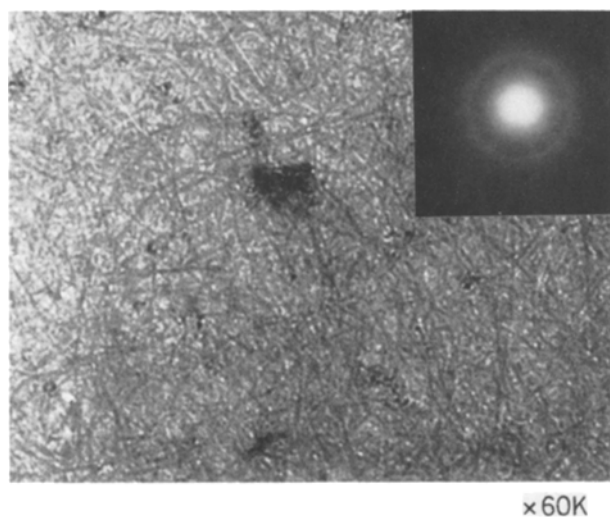
which used only one of the four available 102 reflections.

#### *Morphology of unoriented samples*

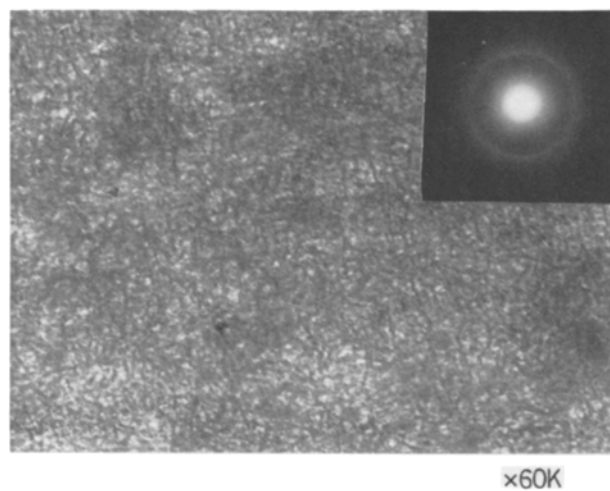
The work described above was all carried out on oriented *i*-PS gels. The electron microscope study of these gels was undertaken in order to identify the morphological features which gave rise to X-ray

patterns observed in oriented gels. However, we need to know whether the effects observed are general to gels, or whether they are largely, or wholly, an effect of orientation. To investigate this, thin films of unoriented gel were studied in the electron microscope.

Thin unoriented gel films were prepared from trans decalin. Thin films were cast from 5% solution of *i*-PS in trans decalin onto cold decalin. After leaving for two days in a refrigerator thin parts of the film were



a



b

Fig. 21. (a) Transmission electron micrograph of a thin film of unoriented unannealed *i*-PS gel cast from trans-decalin. Magnification sixty thousand. Electron diffraction pattern inset (b) Transmission electron micrograph of a thin film as in figure 21a, but accidentally slightly oriented in preparation. Magnification sixty thousand. Electron diffraction pattern inset

picked up on grids. These were found suitable for transmission electron microscopy.

The thin, unoriented films showed a characteristic diffraction pattern and morphology (fig. 21a). The diffraction pattern was a diffuse halo with sharp inner edge (at  $\sim 0.5$  nm) whilst the morphology resembled a tangle of fibres. Where the sample was accidentally slightly oriented the diffraction pattern was intensified along the stress direction (the halo is less pronounced in this direction) and the individual gel films showed a tendency to align (fig. 21b). The connection between the unoriented morphology, the somewhat oriented morphology and the oriented section seen in figure 18b is clear, but there is a difference in that the oriented gel in figure 18b has a finer structure. The diffraction patterns (cf. figs. 21a, 21b and 17a) are, clearly, closely related.

On heating this films of unoriented gel to  $90^\circ\text{C}$  the gel diffraction pattern vanished, as was the case with oriented material. The rate at which the gel diffraction vanished depended on the temperature of annealing; at  $120^\circ\text{C}$  it lasted only about a minute. Soon after the disappearance of the gel diffraction pattern the characteristic sharp ring pattern of the  $3_1$  helix began to emerge and sheaves of  $3_1$  helix crystals appeared and grew. The growth rate of these crystals varied very widely with crystallization temperature. A typical, fully crystallized, area is seen in figure 22a. These sheaves appear to have the same origin as the transverse platelets in figure 18, i. e. they were nucleated by the original gel fibre, except, that being in a random orientation, without the precedent of the oriented structure in figure 18 this is not as apparent by inspection. Nevertheless, in reality the nucleating influence of the initial gel structure is reinforced by its effect on the overall crystallization rates to which we shall now turn.

#### *The effect of the gel structure on nucleation*

We have seen from the DSC studies that the crystallization in the conventional  $3_1$  helix form was much accelerated in samples which have gone through the gel crystal phase. The morphological characteristics of this accelerated crystallization was examined by electron microscopy. The main body of this work will form a separate paper [19]. Here only a brief summary will be added as this is relevant also to the repetition [omet] subject of the present paper.

The overall crystallization rate is determined by two factors, nucleation and growth rate of the crystals. The objective of this part of the electron microscope



×20K

a



×20K

b

Fig. 22. (a) Transmission electron micrograph of a thin film prepared as that in figure 21a and annealed in the electron microscope for 10 minutes at 150 °C. Magnification twenty thousand (b) Transmission electron micrograph of a thin film of *i*-PS prepared as that in figure 22a but held at 225 °C for 5 mins (to reduce the number of crystal nuclei) prior to crystallization for 10 minutes at 150 °C. Magnification twenty thousand

study was to identify which of the two is responsible for the anomalously high overall crystallization rate in samples having passed through the gel state. It was found that the growth rate of the  $3_1$  helix crystals was very similar to that reported by other authors [20, 21] who took optical micrographs of *i*-PS spherulites. However, it was the number of nuclei from which crystals grew that was considerably increased when the sample was heated up from the gel state in comparison with when it was heated up from the

amorphous state. Even when the gel had ceased to diffract (e. g. at 150 °C heating from the gel at 10° per minute) it retained its ability to nucleate  $3_1$  helix crystals. Under the most favourable conditions 24 times as many  $3_1$  helix crystals could be nucleated at 175 °C from an area of film heated from the gel state compared with film heated, under the same conditions, from the amorphous state, and 40 times as many crystals could be obtained by crystallizing the sample from the gel (compared with crystallizing from the amorphous state) at 120 °C. Thus the accelerated crystallization seen (e. g. in DSC, see below) on crystallizing from the gel state is a result of enhanced nucleation.

The nuclei, arising from the gel, could be destroyed by holding the sample at high temperatures. This point is illustrated by figures 22a and 22b. Figure 22a shows a sample crystallized at 155 °C after heating from the gel state at 10° per minute. The same sample was then heated to 225 °C and held there for 5 minutes to destroy all crystallinity. On recrystallization at 155 °C the growth rate of crystals was found to be the same as from the gel nuclei, but the number of crystals was strikingly reduced (fig. 22b). The few nuclei remaining after heating to 225 °C are thought to be heterogeneities, due to particles of catalyst etc.

In summary, the gel material ceases to diffract at 90–120 °C. However, some order is retained and the ordered material provides nuclei from which  $3_1$  helix crystals are able to grow. The enhanced  $3_1$  helix crystal growth, observed when gels are heated, e. g. in the DSC is a result of numerous nuclei, left from the gel phase, being available for growth. The growth rate of individual  $3_1$  helix crystals is no different from that observed from the amorphous phase, but the number of crystals is much increased. The gel nuclei can be destroyed by prolonged heating at high temperatures (e. g. 5 mins at 225 °C) but many remain in a typical 10° per min DSC heating run at the temperatures at which  $3_1$  helix crystal growth is fast.

The infra-red results, reported in the earlier section, are at least consistent with the above finding. Namely, they have revealed the existence of gel crystals at temperatures as high as 150 °C where they have already melted as registered by other, apparently less sensitive, tests. Thus the combined electron microscope and infra-red evidence support each other in as far as the persistence of gel crystal nuclei.

### Summarizing remarks

As stated in the introduction the principal objective of the work was the morphological identification of

the crystal constituents of the thermoreversible *i*-PS gel system. As laid out previously this system is of importance for various reasons. First, it represents a model of thermoreversible crystal gels, a product of a mode of crystallization which since recently has been recognized as widespread in the polymer field displaying several features of general validity. Thus in *i*-PS the competition of the mode of gel crystallization with the more familiar lamellar crystallization is particularly clear cut, the two mutually perpendicular crystal orientations which set in on stretching being one of its consequences. In addition, *i*-PS presents us with a unique situation, namely that the gel forming crystals have a different chain conformation from the conventional three-fold helix. This is of substantial interest *per se*, hence so is any additional information which can be provided on the underlying crystals. Although this new gel structure makes *i*-PS gels special in some respect, in other respects, it provides a valuable aid in the form of a specific fingerprint for the morphological identification of the different texture elements.

All our previous work was on macroscopic samples. To identify electronmicroscopic information with macroscopically registered effects a full coordination of all the relevant techniques was required to ensure that the electron microscopy is representative. This is the primary reason why electron microscopy was preceded and, in some cases, accompanied by several other investigations. We hope that these studies will set a pattern for such a coordinated approach in the future. In addition to being aids for the electron microscopy, each of the techniques employed (X-ray diffraction, DSC and infra-red spectroscopy) provided also varying amounts and kinds of new information on their own. If some questions have remained unanswered this has to be set against the complexity of the system and the problems this poses in a style of investigation which is still in a formative state.

One of the principle problems in the investigation of crystal gels is posed by the fact that the polymer is only a minority component in the wet gel system. Most investigations on the structure, diffraction and imaging, have to be carried out on dry samples. It has been the great merit of the infra-red part of this study to have followed the system through various stages of drying and to ensure that the structures under examination in the partly or fully dried state were representative, in fact quantitatively unaffected by the drying process. In view of the fact that *i*-PS is crystallizable, this quantitative preservation of the structures as originally formed in the wet state on drying, and this without any additional overlay is most fortunate and is probably a unique advantage offered by *i*-PS

compared to other gel forming polymers. DSC offered another suitable bridge between the wet and dried states, even if here the various effects were transposed to higher temperatures on drying.

Before the actual conclusions from this and previous works can be generalized a further safeguard is required. Namely, most information in the past, and largely in the present work, was obtained in the oriented state where the effects in question were most clearly identifiable. In the present work, as was seen, we could ensure that these effects were not produced by stretching and were essentially present already in the random state thus justifying the generalization from oriented samples.

After these reassurances we can proceed to a brief recapitulation of the main results. The gel forming crystal texture was identified as a fibrous mat, or a set of parallel fibrils on orientation (figs. 18, 21). Platelet crystals such as were present initially could be identified, orienting, as anticipated, with their planes along the draw direction (fig. 18a). The latter in itself should be responsible for the perpendicular cross orientations generally observed in stretched gels, and indeed previously unaccounted for diffraction features (the sharp meridional reflexion at 0.629 nm in fig. 1) now in fact falls readily in line. Transformation of the gel structure into the  $3_1$  helix structure could now be identified morphologically (fully backed by the parallel X-ray diffraction, DSC and infra-red studies). It clearly corresponds to parallel platelet structures nucleated by the gel fibres. While the gel fibres themselves seem to melt out according to the combined diffraction and DSC evidence, there are sufficient of them present to act as nuclei when the  $3_1$  helix platelets form. For the latter, minute quantities may suffice, such as detectable only by the infra-red technique and the nucleation memory, as manifest by accelerated crystallization. Whenever the two crystal types, the gel forming and the  $3_1$  helix, are present in sufficient strength to be revealed by diffraction the two are situated in different electron microscopically identifiable localities in the field of view. The platelet structure is clearly manifest as shish-kebab components in the case of oriented samples, testifying further to the fact that they have been nucleated by underlying fibrous entities (figs. 18c, 18e). (The sheave structures forming in random gels can be considered as being of the same origin but with layers parallel only along limited length). The cross orientation revealed by the X-ray patterns in a particularly pronounced form in some heat annealed samples has now found morphological explanation in the orthogonal arrangement of sheaves or whole shish-kebabs (figs. 18d and 20c). We can only surmise

that they are more developed versions of perpendicular lamellar orientation present initially.

The low angle X-ray reflections are fully consistent with the platelet stacking periodicity, falling in line with experience on shish-kebab type structures in general. The conversion of fibres to platelets is fully consistent also with the change from narrow to broad X-ray line width of the appropriate meridional (or nearly so) reflections, a feature noted previously [2] but without the morphological back-up now provided.

It is apparent from all the above that the change from the gel structure to the  $3_1$  helical structure is not a straightforward crystal phase transformation but proceeds via melting and recrystallization. Nevertheless, the two processes are interrelated via the nucleating influence of the residues of the original gel structure.

The last mentioned feature is strikingly manifest through the accelerated overall crystallization of the  $3_1$  structure in samples which have gone through gelation originally, whether after passing through the gel phase, or even after complete melting of the resulting  $3_1$  helical crystal phase, provided holding time in the melt was short. It was established (and to be reported on in detail later [19]) that this accelerated crystallization is due to the enhanced number of nuclei (and not to increased crystal growth) in such samples. As known, *i*-PS normally crystallizes very slowly which is one of the main limitations to its technological application as a crystalline thermoplastic. Its intrinsic interest apart, a method which can speed up crystallization should therefore merit attention.

So far we have not commented on the nature of the novel gel crystal structure itself, the subject of most previous publications on this topic. To recall, its interest stems from the extended near all  $TT$  chain conformation giving rise to it. While not the main subject of this study a certain amount of noteworthy new information has emerged. One of these is the significant infra-red result that the chain conformation, as diagnosed by the characteristic gel bands, are identical for gel crystals formed from both trans and cis decalin in spite of the notable difference in their respective X-ray diffraction patterns. This confirms our previously expressed view that we are dealing with identical chain conformations but in different chain packings, possibly also influenced by the presence of the solvent. In the latter respect we reconfirmed by X-ray and electron diffraction, by DSC calorimetry and by infra-red spectroscopy that the gel structure can exist completely dry, hence contrary to assertions by Sundararajan [10] the extended chain near all  $TT$  conformation does not depend on a solvent for its

existence, although it does so in its formation. Thus, attempts to account for the crystal structure by placing solvent molecules in the unit cell are misplaced at least in the case of the gel as obtained from trans decalin. However, we admit that the presence of solvent can influence the chain packing and the corresponding features in the diffraction pattern in the case of gels from certain solvents. Thus the X-ray pattern characteristic of gels from cis decalin cannot exist solvent free: if solvent is extracted it gives way to the  $3_1$  helical structure as reported previously, and under circumstances, as found in the present work, can transform into the near all  $TT$  pattern characteristic of gels from trans decalin. Accordingly, the diffraction pattern corresponding to the latter should be the one which is intrinsic to the extended near all  $TT$  conformation itself.

#### Acknowledgements

We thank the Science and Engineering Research Council for support.

#### References

1. Keller A (1983) in Structure-Property Relationships of Polymeric Solids Ed Anne Hiltner Plenum Press New York p 25
2. Girolamo M, Keller A, Miyasaka K, Overbergh N (1976) *J Polym Sci (Polym Phys Edn)* 14:39
3. Atkins EDT, Isaac DH, Keller A, Miyasaka K (1977) *J Polym Sci (Polym Phys Edn)* 15:211
4. Atkins EDT, Isaac DH, Keller A (1980) *J Polym Sci (Polym Phys Edn)* 18:71
5. Atkins EDT, Keller A, Shapiro JS, Lemstra PJ (1981) *Polymer* 22:1161
6. Natta G, Corradini P, Bassi IW (1960) *Nuovo Cimento Suppl* 1 15:68
7. Sundararajan PR (1979) *Macromol* 12:575
8. Corradini P, Guerra G, Petracone V, Pirozzi B (1980) *Eur Polym J* 5:1089
9. Atkins EDT, Keller A (to be published)
10. Sundararajan PR, Tyrer NJ, Bluhm TL (1982) *Macromol* 15:286
11. Sundararajan PR, Tyrer NJ (1982) *Macromol* 15:1004
12. Painter PC, Kessler RE, Snyder RW (1980) *J Polym Sci (Polym Phys Edn)* 18:723
13. Guerrero SJ, Keller A, Soni PL, Geil PH (1980) *J Polym Sci (Polym Phys Edn)* 18:1533
14. Berghmans H, Overbergh N, Gavearts F (1979) *J Polymer Sci Phys Ed* 17:1251
15. Kobayashi M, Tsumura T, Tadokoro H (1968) *J Polymer Sci A-2* 6:1473
16. Wellinghoff S, Shaw J, Baer E (1982) *Macromol* 15:464
17. Helms JB, Challa G (1972) *J Polym Sci A-2* 10:761
18. Hill MJ, Keller A (1971) *J Macromol Sci* 5:591

19. Hill MJ, Keller A to be published
20. Suzuki T, Kovacs A (1970) *Polym Journal* 1:82
21. Boon J, Thesis PhD (1966) University of Delft

Received May 3, 1983;  
accepted Juli 20, 1983

Authors' address:

E. D. T. Atkins  
H. H. Wills Physics Laboratory  
University of Bristol  
Tyndall Avenue  
Bristol BS8 1TL (U. K.)